Silver Nanowire−Conducting Polymer−ITO Hybrids for Flexible and Transparent Conductive Electrodes with Excellent Durability

Ji Hoon Yoo,[†,‡,§] Yunkyung Kim,[†,#] Mi Kyoung Han,[§] Seonghwa Choi,[#] Ki Yong Song,[§] Kwang Choon Chung,[§] Ji Man Kim,*[,‡] and Jeonghun Kwak*[,#]

‡Department of Chemistry, Sungkyunkwan University, Suwon 440-746, South Korea
§InkTec Co. Ltd, Ansan-si, Gyeonggi-do 425-839, South Korea
#Department of Electronic Engineering, Dong-A University, Busan 604-714, South Korea

Ⓢ *Supporting Information*

ABSTRACT: Solution-processed silver nanowire (AgNW) films have attracted attention as transparent and conductive electrodes for flexible optoelectronic devices and touch screens, to replace sputtered indium−tin-oxide (ITO) films. However, the mechanical flexibility, environmental durability, and the optical (such as transparency and a haze) and electrical properties of the AgNW films should be improved for their practical application. In this work, high-performance and roll-to-roll processed AgNW-based hybrid electrodes comprising poly(3,4-ethylenedioxythiophene):poly(styrenesulfonate) (PE-DOT:PSS) and/or ITO are introduced. The optical and electrical properties of the AgNW films combined with PEDOT:PSS, ITO, or both of them were systematically examined. Among the films, the AgNW−PEDOT:PSS−ITO hybrid film exhibits a high transmittance (88%) and a low sheet resistance (44 Ω sq^{-1}) with a small haze (1.9%). Moreover, the hybrid films show excellent durability to a variety of environmental stresses. By virtues of the high performance and durability, it is believed that the AgNW−PEDOT:PSS−ITO hybrid electrodes are highly suitable for practical use.

KEYWORDS: *transparent conductive electrodes, silver nanowires, flexible electrodes, hybrids, durability*
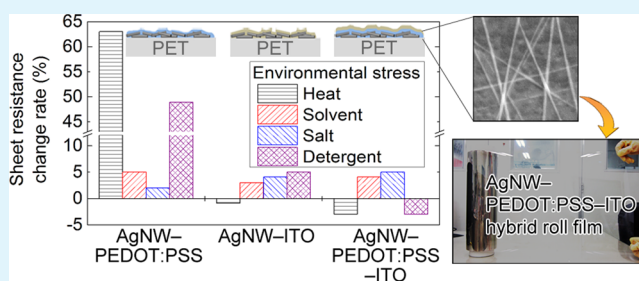
INTRODUCTION

Recently, the development of highly flexible, transparent, and conductive electrodes has grown in importance due to the increasing industrial demands for their application to flexible displays and touch screen films. For these devices, transparent conducting oxides, represented by indium−tin-oxide (ITO), have been the most widely used so far. However, despite the high electrical conductivity and optical transparency of the ITO, it is not applicable to plastic-based flexible devices because the ITO electrodes crack into small pieces by durational bending.[1] Great efforts have been devoted to the research on transparent and flexible electrodes to replace the ITO. Several alternatives have been introduced based on conducting polymers (e.g., polyaniline and poly(3,4-ethylenedioxythiophene):poly(styrenesulfonate) [PE-DOT:PSS]),[2−4] 2D/3D carbon allotropes (e.g., graphene and carbon nanotubes),[5,6] silver nanowires (AgNWs),[7−29] and their complexes. Among them, randomly distributed AgNWs are considered as the most promising candidate for the electrodes, because they exhibit superior transparency and mechanical flexibility, compared to the others.[7−9] In addition, they can be processed on glass, plastics, and papers[10,11] at low temperature (<200 °C) with various deposition methods, such as spin-coating, spray-coating, bar-coating, screen-printing, transfer-printing, and so on.[12−14]

On the other hand, to utilize AgNW films as the electrodes of optoelectronic devices, it is required to decrease the surface roughness of AgNW films originating from the thread shape of a single nanowire and their random distribution within films. The rough surface of the AgNW films decreases the uniformity in their electrical and optical properties, resulting in a short circuit or a haze in devices and films. In addition, pristine random AgNW networks show lower electrical conductivity than expected because of the poor interconnection between wires. An insulating capping layer (e.g., polyvinylpyrrolidone), which was employed to control the size of the AgNWs during synthesis and to disperse them, also obstructs the migration of charge carriers between the nanowires.[7−9,15,16] To reduce the contact resistance, various methods have been introduced, such as soldering/welding the AgNW junctions,[17−19] and embedding the AgNWs in PEDOT:PSS,[20−22] metal oxides,[23−25] or graphene.[26−28] These methods extend the contact area between AgNWs, leading to an improvement in electron conduction. Also, the surface morphology can be smooth by filling the gaps between AgNWs. But at the same time, there are drawbacks of the methods. For instance, adding PEDOT:PSS to AgNW films

reduces the optical transparency due to the light absorption over the visible−NIR spectral range. Adding metal oxide layers and partial soldering/welding of the AgNWs can decrease the uniformity and increase the haze of the film.

Moreover, the flexibility and durability of the AgNW films to a variety of environmental stresses should be examined for their practical application. Numerous studies have introduced the methods toward improving the performance of AgNW electrodes in terms of the electrical conductivity, optical properties, and processability, but only a small minority of them have investigated the durability of the electrodes.

In this work, we introduce roll-to-roll (R2R) processed hybrid electrodes on plastic films by incorporating PEDOT:PSS into AgNWs and an additional very thin ITO layer. Through a systematic investigation of the performance of the AgNW, AgNW−PEDOT:PSS, AgNW−ITO, and AgNW−PE-DOT:PSS−ITO hybrid electrodes, we found that the AgNW−PEDOT:PSS−ITO electrodes exhibited excellent flexibility and durability to a variety of mechanical, thermal, and chemical stresses, as well as high transparency, a small haze, and a low sheet resistance. The high performance of the hybrid films were attributed to the high resistance of the ITO to the environmental stresses and the improved interconnection by PEDOT:PSS. Optical simulation results also verified the enhancement of the optical properties in the hybrid electrodes.

■ RESULTS AND DISCUSSION

As described previously, the performance of AgNW thin-films can be improved by adding conductive materials. Considering the electrical conductivity, optical transparency, and practical processability, PEDOT:PSS and ITO were selected as the supporting materials for AgNWs. As shown in Figure 1, four kinds of flexible, transparent, and conductive films were fabricated via the R2R process, which were AgNW, AgNW−PEDOT:PSS, AgNW−ITO, and AgNW−PEDOT:PSS−ITO. In detail, AgNW and AgNW−PEDOT:PSS composite films were formed on a flexible polyethylene terephthalate (PET) film by slot-die coating the AgNW and AgNW−PEDOT:PSS composite inks. For the ITO-added films, a thin ITO layer was sputtered onto the AgNW or AgNW−PEDOT:PSS composite film also by the R2R process. The schematic illustration of the procedures and the photograph of the fabricated hybrid film roll are displayed in Figure 1.

First, we fabricated the AgNW−PEDOT:PSS films with varying the solid (dry) weight ratio of PEDOT:PSS to AgNW as 1:2, 1:1, and 3:1 and compared the electrical and optical properties. As shown in Table 1, the initial R_S of the pristine AgNW film was 48.3 Ω sq^{-1} with a standard deviation of 0.70 Ω sq^{-1}, while that of AgNW−PEDOT:PSS (1:2) film was slightly decreased to 46.3 Ω sq^{-1} with a standard deviation of 0.64 Ω sq^{-1}. The values were decreased steadily as the ratio of PEDOT:PSS to AgNW was increased, which is a trend similar to that of a previous report on AgNW−PEDOT:PSS composite films.[14] Because the surface scanning electron microscope (SEM) images of the films with various PEDOT:PSS ratios show no considerable difference (Figure S1, Supporting Information), we think that PEDOT:PSS homogeneously infiltrated into the gaps between AgNWs and increased the percolation paths for charge carriers. The addition of PEDOT:PSS into AgNW also improved the mechanical flexibility of the films. Here, to present the mechanical reliability, we defined the relative change in electrical resistance (ΔR) as
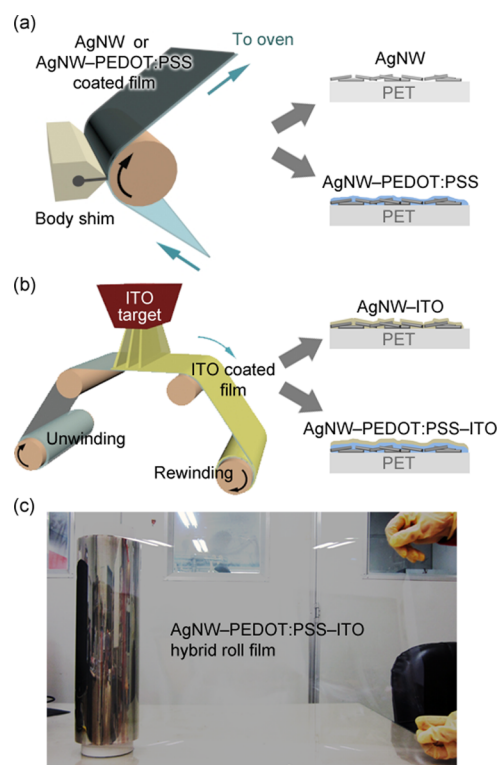
Figure 1. Schematic diagrams of the R2R processes with (a) the slot-die coating for the AgNW and AgNW−PEDOT:PSS film, and (b) the ITO sputtering for the AgNW−ITO and AgNW−PEDOT:PSS−ITO films. (c) The photograph of the fabricated AgNW−PEDOT:PSS−ITO hybrid roll film.

Table 1. Electrical and Optical Properties of the Pristine AgNW Film and AgNW−PEDOT:PSS Composite Films

		PEDOT:PSS:AgNW (w/w)		
	pristine AgNW	1:2	1:1	3:1
R_S (Ω sq^{-1})	48.3	46.3	45.2	40.2
ΔR (%)	fail	1.0	0.9	0.7
T (%) @550 nm	91.5	90.2	89.0	87.9
H (%)	1.9	1.9	2.0	2.2

$$\Delta R = (R - R_0)/R_0 \qquad (1)$$

where R_0 and R are the resistances before and after 3000 cycles of bending, respectively. The relative resistance change of the pristine AgNW film was not measurable after a few cycles of bending, whereas the values of the AgNW−PEDOT:PSS composite films were decreased to 1.0, 0.9, and 0.7% as the content of PEDOT:PSS increased. It is attributed to the high flexibility of the polymeric material, PEDOT:PSS. On the other hand, the optical properties were degraded by blending AgNW with PEDOT:PSS. The transmittance (T) of the pristine AgNW film measured at 550 nm was 91.5%. But it was lowered to 87.9% as the ratio of PEDOT:PSS increased. The results can be explained by the wide optical absorption property of the PEDOT:PSS film over the entire visible ranges. Simultaneously, the haze (H) was increased from 1.9% to 2.2%. In other words, the addition of PEDOT:PSS to AgNW enhances the electrical and mechanical properties but decreases the optical properties.

Subsequently, we investigated the performance of ITO-added AgNW films. Although ITO films are brittle during repetitive bending, they have irreplaceably good electrical and optical

properties for transparent conducting electrodes. Thus, depositing a thin ITO layer onto AgNW films can improve the electrical properties without loss of their optical properties. By the R2R-based sputtering process, we fabricated the AgNW–ITO films with an ITO thickness of 10, 20, 30, or 40 nm and compared their performance with that of the pristine AgNW film. As shown in the SEM and atomic force microscopy (AFM) images in Figure 2, the widths of AgNWs
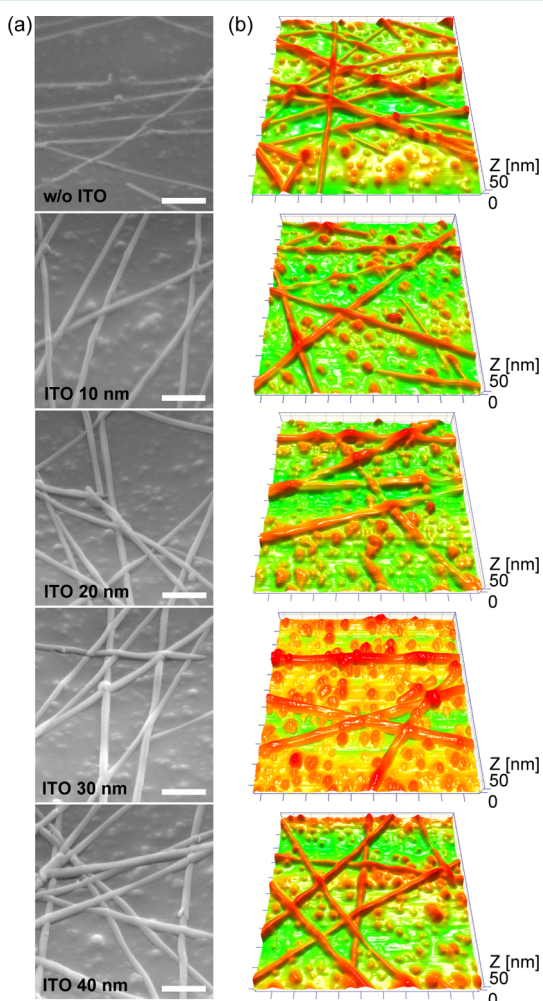
Figure 2. (a) SEM images (scale bar: 500 nm) and (b) AFM images (5 μm × 5 μm) of the AgNW–ITO composite films with various ITO thicknesses (0–40 nm).

were widened to about 60–80 nm as the ITO thickness was increased, meaning that ITO covered each AgNW homogeneously. The average surface roughness of the pristine AgNW film was 12.4 nm, while the values of the ITO-added films were increased to 15.3–18.0 nm. As expected, the electrical properties of the ITO-added films were better than that of the pristine AgNW film and the AgNW–PEDOT:PSS composite films (Table 2). The R_S was reduced to 44.2, 34.1, 25.0, and 22.2 Ω sq^{-1} when the thickness of the ITO was 10, 20, 30, and 40 nm, respectively. However, the addition of ITO to AgNW diminished the mechanical stability, causing a ΔR (2–298% depending on the ITO thickness) much higher than that of the films without ITO. The film with a 10 nm ITO layer exhibited an optical transmittance as high as 90.5% at 550 nm. As the thickness of ITO was increased, the transmittance was

**Table 2. Electrical and Optical Properties of the AgNW–ITO Films Depending on the ITO Thickness**

	thickness of ITO on AgNWs (nm)			
	10	20	30	40
R_S (Ω sq^{-1})	44.2	34.1	25.0	22.2
ΔR (%)	2	7	62	298
T (%) @550 nm	90.5	89.5	88.7	86.4
H (%)	2.0	2.3	2.3	2.4

slightly decreased. However, the haze was rapidly increased from 1.9% (in the pristine AgNW film) to 2.0–2.4% when 10–40 nm of the ITO layer was deposited onto the films.

On the basis of the systematic investigation of the properties of AgNW films with PEDOT:PSS or ITO, we fabricated novel hybrid electrodes with AgNW–PEDOT:PSS–ITO films which exhibit good electrical, optical, and mechanical performance. Here we fixed the weight ratio of PEDOT:PSS to AgNW as 1:2 by considering the trade-off between electrical and optical properties along with the PEDOT:PSS content as shown above. The ITO thickness was precisely tuned to 8, 10, and 15 nm to find the optimum thickness for the lower haze and ΔR. Figure 3(a) and 3(b) show the SEM and AFM images of the AgNW–PEDOT:PSS–ITO hybrid films with various thicknesses of ITO. The average width of the AgNWs with a 10 nm ITO layer was about 60 ± 10 nm, but that in the AgNW–PEDOT:PSS–ITO hybrid films with the same ITO thickness was observed as 55 ± 8 nm because the AgNWs were partly buried under PEDOT:PSS. The average surface roughness was in the range of 11.7–15.0 nm, which are slightly lower than the values of the films without PEDOT:PSS.

The electrical properties of the hybrid films with the various ITO thicknesses are displayed in Figure 3(b). Similar to the results of the AgNW–ITO experiment above, the R_S was decreased as the ITO thickness was increased. Moreover, as shown in the graph with box-and-whisker plots (from the measurement of 36 different points), the homogeneity of the R_S was improved with the additional ITO layer. The interquartile range (IQR) values (defined as IQR = first quartile–third quartile of data) were reduced to 1.3, 1.0, and 0.5 Ω sq^{-1} for the hybrid films with the 8, 10, and 15 nm of ITO layer, respectively, while that of the film without additional ITO layer was 0.7 Ω sq^{-1}. Interestingly, the addition of ITO also improved the mechanical flexibility of the electrodes. The ΔR was 1.0% without ITO, and it was decreased to 0.5% with an 8 nm ITO layer. The value was increased to 0.7% with the ITO thickness of 10 and 15 nm, but it was still lower than that without ITO. It may be attributed to the use of both PEDOT:PSS and ITO. They can not only enhance the interconnection between AgNWs but can also redeem the defects (e.g., coverage) from each other.

Although the optical transmittance slightly decreased when an ITO layer was added as shown in Figure 3(c), the decrement was small. The transmittance of the hybrid films with 8, 10, and 15 nm of the ITO layers was 89.5%, 89.4%, and 87.7%, respectively, which is higher than the values of the AgNW films with a high content of PEDOT:PSS showing comparable electrical performance. Also, we found that the deposition of ITO onto the AgNW–PEDOT:PSS films did not increase the haze of the films in contrast with the AgNW–ITO films. The measured haze values, 1.9%, were maintained for all the ITO thicknesses, which are the same values as those of the pristine AgNW film and the AgNW–PEDOT:PSS film without ITO.
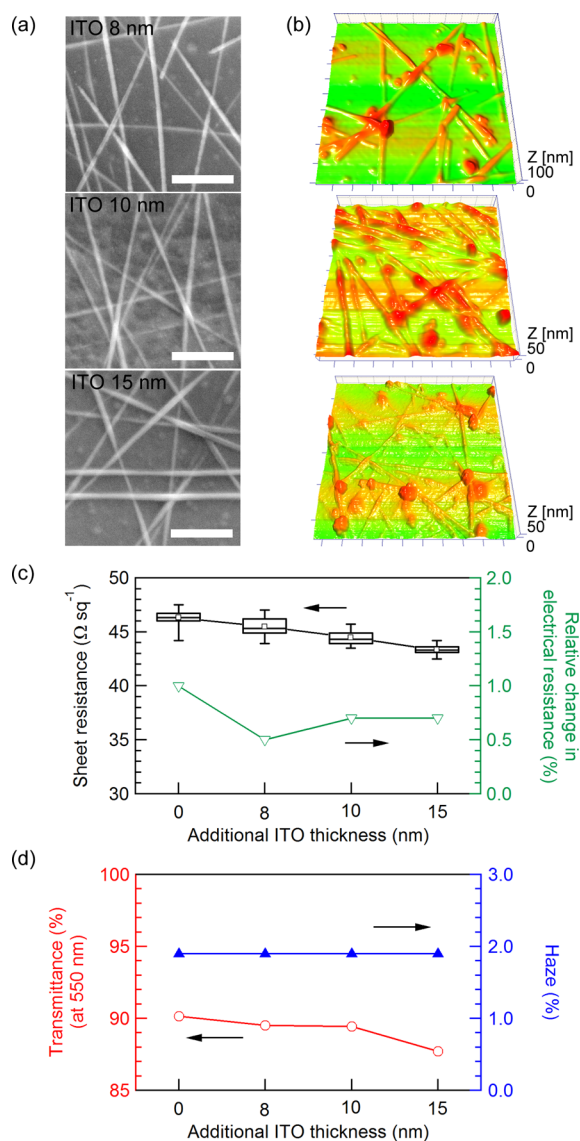
Figure 3. (a) SEM images (scale bar: 500 nm) and (b) AFM images (5 μm × 5 μm) of the AgNW−PEDOT:PSS−ITO hybrid films with the various ITO thicknesses and their electrical/optical properties in terms of (c) the sheet resistance and the relative change in electrical resistance and (d) the optical transmittance at 550 nm and a haze.

As mentioned in the introductory part, transparent and conductive electrodes need to have a low haze as well as good electrical conductivity because they usually locate in front of displays transmitting light. Therefore, we believe that the development of the AgNW−PEDOT:PSS−ITO hybrid films exhibiting improved electrical and mechanical performance with little optical loss is meaningful and encouraging for the practical use of AgNW-based electrodes.

To understand the mechanism for the good hazes in the AgNW−PEDOT:PSS−ITO hybrid films regardless of the ITO layer, the optical properties of the AgNW−ITO film and AgNW−PEDOT:PSS−ITO hybrid film were investigated by optical simulation. The finite-difference time-domain (FDTD) method is generally used for a numerical analysis on the scattering cross section of individual cylindrical nanowires.[29,30] In our calculation, two-dimensional total scattered field was used. The incident light of wavelength between 400 and 800 nm propagates in the direction of the y-axis. The TE and TM

polarization modes are simulated, and the average results of them are used. The mesh size was set to 0.5 nm. Complex refractive indices (n, k) of ITO and PEDOT:PSS used in the numerical calculation were obtained by variable angle spectroscopic ellipsometry. The optical constants of the Ag and PET were acquired from the literature.[31,32] The structures of the simulated films for the AgNW−ITO and AgNW−PEDOT:PSS−ITO hybrid films are shown in Figure 4(a) and
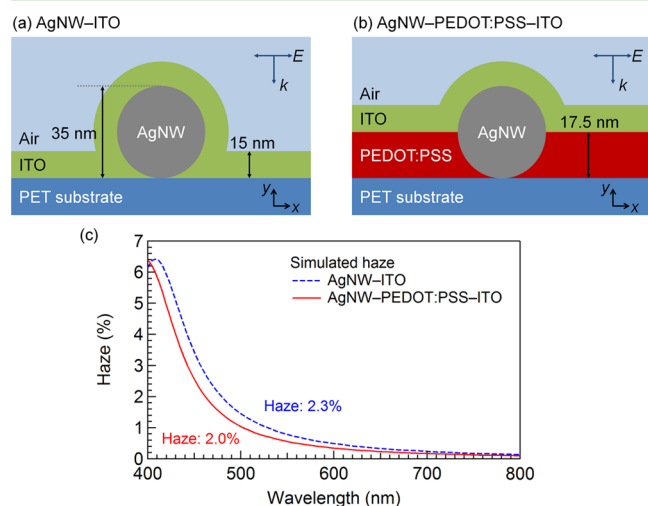

Figure 4. Schematics of the 2D FDTD simulation structures for the (a) AgNW−ITO film and (b) AgNW−PEDOT:PSS−ITO hybrid film, and (c) the calculated hazes of two structures.

4(b), respectively. An AgNW with a diameter of 35 nm was placed on the PET substrate. For the hybrid film, we configured the thickness of the PEDOT:PSS layer as half of the AgNW diameter because PEDOT:PSS infiltrated into the gaps between AgNWs. The thickness of the ITO layer covering both films was set to 15 nm. The haze is defined as[29]

$$haze = \frac{\text{forward scattered light}}{\text{forward nonscattered light} + \text{forward scattered light}}$$

$$(2)$$

where the forward light indicates the power that resides in the substrates passing through the AgNWs. The simulation results of the haze for two films are compared in Figure 4(c). For the wavelengths of above 420 nm, the haze of the AgNW−ITO is larger than that of the AgNW−PEDOT:PSS−ITO hybrid film. Also, the haze peak of the AgNW−ITO was slightly red-shifted from that of AgNW−PEDOT:PSS−ITO. It may be attributed to the difference of refractive indices between ITO and PEDOT:PSS which are surrounding the AgNWs. A previous report showed that the scattering intensity peak shifted to longer wavelengths, as the adjacent medium had a higher refractive index.[33] In our case, the refractive index of ITO is higher than PEDOT:PSS. As a result, the average haze of the AgNW−ITO film (2.3%) is higher than that of the hybrid film (2.0%). In other words, the haze was reduced with the addition of PEDOT:PSS. It also supports the above results of the same hazes in the AgNW−PEDOT:PSS−ITO hybrid film irrespective of the ITO thickness.

The electric field distributions in the xy-plane at the peak of scattering cross section (at λ = 408 nm) for the two AgNW films are shown in Figure 5(a) and 5(b) for observing the
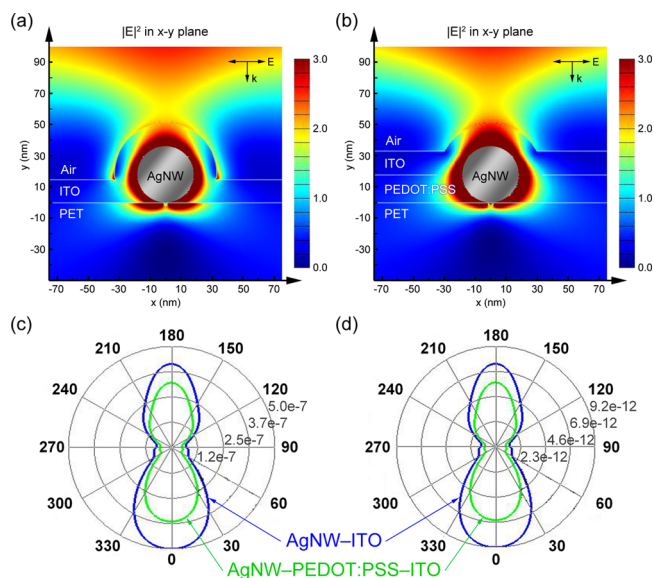
Figure 5. (a, b) Calculated electric field distributions in *xy*-plane at the peak of scattering cross section (at λ = 408 nm) of each structure for the (a) AgNW−ITO film and (b) AgNW−PEDOT:PSS−ITO hybrid film. (c, d) Simulation of the scattered field intensity versus scattering angle for (c) TE polarization and (d) TM polarization in linear scale.

degree of light propagation into the substrate. As shown in the figures, the electric field intensity of the AgNW−ITO film within the PET substrate is larger than that of the AgNW−PEDOT:PSS−ITO film. It means that the light scattering is increased in the AgNW−ITO film, resulting in an increase of the haze. Further analysis of the scattered field intensity in both films with respect to the scattering angle is shown in Figure 5(c) and 5(d) for the TE and TM polarization modes, respectively. The forward scattering is represented by angles 0−90° and 270−360°, and the backscattering is represented by 90−270°. The simulation results show that the highest field intensities propagate forward and in return for both TE and TM polarizations. The scattering intensity of the AgNW−ITO film is larger than that of the AgNW−PEDOT:PSS−ITO hybrid film for both TE and TM polarizations. The forward scattering of the AgNW−ITO film is also larger than that of the other. It corresponds to the electric field distribution, which explains the reason for smaller hazes in PEDOT:PSS embedded films.

Finally, the durability of the AgNW-based electrodes to various environmental stresses, i.e., heat, solvent, detergent, and salt, were investigated. It was examined by measuring the sheet resistance before (R_{S0}) and after (R_{SS}) the stress, and then the relative change in sheet resistance (ΔR_S) was calculated as

$$\Delta R_S = (R_{SS} - R_{S0})/R_S \quad (3)$$

For the thermostability test, the films were annealed under an ambient air condition at 80 °C for 120 h. For the tests of the resistance to solvent, detergent, and salt, the films were immersed into 98% ethanol for 30 min, 5 wt % commercially available neutral detergent aqueous solution for 3 h, and 10 wt % NaCl solution for 3 h, respectively. After that, the films were softly rinsed with deionized water to measure the sheet resistance. As summarized in Table S1 in Supporting Information, we failed to measure the R_{SS} in the pristine AgNW films for all stress conditions. Although we could not obtain any evidence for the poor durability of the pristine

AgNW film by observing the surface morphology and X-ray diffraction, it may be attributed to the oxidation of AgNWs and/or weak adhesion between AgNWs and substrates. Also, the Cl⁻ ions in NaCl solution can react with Ag. In the other films, we can measure the ΔR_S as shown in Figure 6. The R_{SS} of
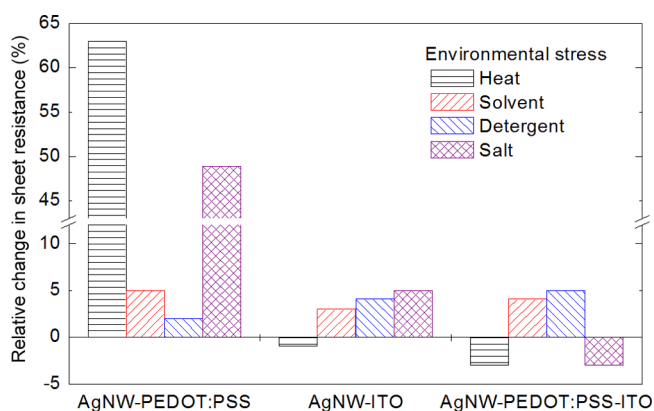
Figure 6. Relative change in sheet resistance of the AgNW−PEDOT:PSS, AgNW−ITO, and AgNW−PEDOT:PSS−ITO films under various types of environmental stress.

the AgNW−PEDOT:PSS film was considerably changed by the heat and NaCl. Because PEDOT:PSS could not fully cover each AgNW as shown in the SEM images (Figure S1, Supporting Information), AgNWs were likely to be oxidized. Nevertheless, PEDOT:PSS improved the resistance to the solvents and solutions by increasing the intra- and interconnection of AgNW−AgNW and AgNW−substrate. Meanwhile, the AgNW−ITO film shows good durability in various tests ($\Delta R_S \leq$ 5%). In this film, a thin ITO layer covers the surface of the AgNW film, preventing the AgNWs from oxidation, detachment, and chemical reaction. The AgNW−PEDOT:PSS−ITO hybrid film also exhibits good durability in all the tests comparable to the AgNW−ITO film owing to the passivation by the thin ITO layer. Therefore, we could obtain excellent durability as well as good electrical, mechanical, and optical properties by the hybridization of three components.

CONCLUSION

We have fabricated highly flexible, conductive, and transparent electrodes by introducing the AgNW−PEDOT:PSS−ITO hybrid films in R2R process. Embedding PEDOT:PSS in AgNW films improved the electrical conductivity and mechanical flexibility of the films due to the enhanced interconnection between AgNWs, whereas it reduced the optical properties. Depositing a thin ITO layer on AgNWs films enhanced the surface resistance, but it made the flexibility poor. By developing the AgNW−PEDOT:PSS−ITO hybrid electrodes, we could overcome the trade-off between electrical, optical, and mechanical properties. The R2R-based hybrid films also showed superior durability to various types of environmental stresses and lower hazes compared to the other AgNW-based films, offering high practicality for electronic applications.

EXPERIMENTAL SECTION

The AgNW ink and PEDOT:PSS (Clevios PH 1000) were purchased from Nanopyxis and Heraeus Precious Metals, respectively. The average width of the AgNWs was 35 nm (30−40 nm). The AgNWs and AgNW−PEDOT:PSS composite inks were formulated by adding a small amount of dispersing agent (BYK Anti-Terra-250, 0.25 wt %),

a polymer binder (hydroxypropyl methylcellulose, 1 wt %), and solvent (5 wt % of isopropyl alcohol in deionized water). The inks were slot-die-coated onto a flexible PET film (125-μm-thick) at the speed of 8 m/min through an R2R system, followed by annealing in an in-line oven at 120 °C for 3 min.

The SEM and AFM images were obtained using a MIRA-1 (Tescan) and a NANOStation-HD (Surface Imaging System), respectively. The sheet resistance (R_S) was measured by the four-point probe method (MCP-T610, Mitsubishi Chemical Analytech). A cyclic bending test was performed with a bending radius of 5 mm using a lab-made test machine consisting of motor-driven mounting stages and a digital multimeter to indicate the real-time resistance. The optical transmittance (T) and a haze (H) of the films were measured with a haze meter (NDH-5000, Nippon Denshoku Industries). For the optical simulation of the scattered light intensity of AgNWs, a commercial optical simulator (Lumerical Solutions, Inc.) was used. Spectroscopic ellipsometry (M-2000D, J.A. Woollam Co.) was used to determine the complex refractive indices of the ITO and PEDOT:PSS layers.

■ ASSOCIATED CONTENT

ⓢ Supporting Information
SEM images and detailed performance table for all films. The Supporting Information is available free of charge on the ACS Publications website at DOI: 10.1021/acsami.5b03855.

■ AUTHOR INFORMATION

Corresponding Authors
*E-mail: jimankim@skku.edu.
*E-mail: jkwak@dau.ac.kr.

Author Contributions
†These authors contributed equally to this work.

Notes
The authors declare no competing financial interest.

■ ACKNOWLEDGMENTS

■ REFERENCES

(1) Sierros, K. A.; Morris, N. J.; Ramji, K.; Cairns, D. R. Stress−Corrosion Cracking of Indium Tin Oxide Coated Polyethylene Terephthalate for Flexible Optoelectronic Devices. *Thin Solid Films* **2009**, *517*, 2590−2595.

(2) Cao, Y.; Treacy, G. M.; Smith, P.; Heeger, A. J. Solution-Cast Films of Polyaniline: Optical-Quality Transparent Electrodes. *Appl. Phys. Lett.* **1992**, *60*, 2711−2713.

(3) MacDiarmid, A. G. Synthetic Metals: A Novel Role for Organic Polymers. *Synth. Met.* **2001**, *125*, 11−22.

(4) Kirchmeyer, S.; Reuter, K. Scientific Importance, Properties and Growing Applications of Poly(3,4-ethylenedioxythiophene). *J. Mater. Chem.* **2005**, *15*, 2077−2088.

(5) Kim, K. S.; Zhao, Y.; Jang, H.; Lee, S. Y.; Kim, J. M.; Kim, K. S.; Ahn, J.-H.; Kim, P.; Choi, J.-Y.; Hong, B. H. Large-Scale Pattern Growth of Graphene Films for Stretchable Transparent Electrodes. *Nature* **2009**, *457*, 706−710.

(6) Gruner, G. Carbon Nanotube Films for Transparent and Plastic Electronics. *J. Mater. Chem.* **2006**, *16*, 3533−3539.

(7) Langley, D.; Giusti, G.; Mayousse, C.; Celle, C.; Bellet, D.; Simonato, J.-P. Flexible Transparent Conductive Materials Based on Silver Nanowire Networks: a Review. *Nanotechnology* **2013**, *24*, 452001.

(8) Liu, C.-H.; Yu, X. Silver Nanowire-Based Transparent, Flexible, and Conductive Thin Film. *Nanoscale Res. Lett.* **2011**, *6*, 75.

(9) Li, X.; Wang, L.; Yan, G. Review: Recent Research Progress on Preparation of Silver Nanowires by Soft Solution Method and Their Applications. *Cryst. Res. Technol.* **2011**, *46*, 427−438.

(10) Preston, C.; Fang, Z.; Murray, J.; Zhu, H.; Dai, J.; Munday, J. N.; Hu, L. Silver Nanowire Transparent Conducting Paper-Based Electrode with High Optical Haze. *J. Mater. Chem. C* **2014**, *2*, 1248−1254.

(11) Zhu, H.; Fang, Z.; Preston, C.; Li, Y.; Hu, L. Transparent Paper: Fabrications, Properties, and Device Applications. *Energy Environ. Sci.* **2014**, *7*, 269−287.

(12) Madaria, A. R.; Kumar, A.; Ishikawa, F. N.; Zhou, C. Uniform, Highly Conductive, and Patterned Transparent Films of a Percolating Silver Nanowire Network on Rigid and Flexible Substrates Using a Dry Transfer Technique. *Nano Res.* **2010**, *3*, 564−573.

(13) Scardaci, V.; Coull, R.; Lyons, P. E.; Rickard, D.; Coleman, J. N. Spray Deposition of Highly Transparent, Low-Resistance Networks of Silver Nanowires over Large Areas. *Small* **2011**, *7*, 2621−2628.

(14) Choi, D. Y.; Kang, H. W.; Sung, H. J.; Kim, S. S. Annealing-Free, Flexible Silver Nanowire−Polymer Composite Electrodes via a Continuous Two-Step Spray-Coating Method. *Nanoscale* **2013**, *5*, 977−983.

(15) Sun, Y.; Gates, B.; Mayers, B.; Xia, Y. Crystalline Silver Nanowires by Soft Solution Processing. *Nano Lett.* **2002**, *2*, 165−168.

(16) Hu, L.; Kim, H. S.; Lee, J.-Y.; Peumans, P.; Cui, Y. Scalable Coating and Properties of Transparent, Flexible, Silver Nanowire Electrodes. *ACS Nano* **2010**, *4*, 2955−2963.

(17) Garnett, E. C.; Cai, W.; Cha, J. J.; Mahmood, F.; Connor, S. T.; Christoforo, M. G.; Cui, Y.; McGehee, M. D.; Brongersma, M. L. Self-Limited Plasmonic Welding of Silver Nanowire Junctions. *Nat. Mater.* **2012**, *11*, 241−249.

(18) Lee, J.; Lee, I.; Kim, T.-S.; Lee, J.-Y. Efficient Welding of Silver Nanowire Networks without Post-Processing. *Small* **2013**, *9*, 2887−2894.

(19) Lee, J.; Lee, P.; Lee, H. B.; Hong, S.; Lee, I.; Yeo, J.; Lee, S. S.; Kim, T.-S.; Lee, D.; Ko, S. H. Room-Temperature Nanosoldering of a Very Long Metal Nanowire Network by Conducting-Polymer-Assisted Joining for a Flexible Touch-Panel Application. *Adv. Funct. Mater.* **2013**, *23*, 4171−4176.

(20) Gaynor, W.; Burkhard, G. F.; McGehee, M. D.; Peumans, P. Smooth Nanowire/Polymer Composite Transparent Electrodes. *Adv. Mater.* **2011**, *23*, 2905−2910.

(21) Kim, S.; Kim, S. Y.; Kim, J.; Kim, J. H. Highly Reliable AgNW/PEDOT:PSS Hybrid Films: Efficient Methods for Enhancing Transparency and Lowering Resistance and Haziness. *J. Mater. Chem. C* **2014**, *2*, 5636−5643.

(22) Kim, S.; Kim, S. Y.; Chung, M. H.; Kim, J.; Kim, J. H. A One-Step Roll-to-Roll Process of Stable AgNW/PEDOT:PSS Solution Using Imidazole as a Mild Base for Highly Conductive and Transparent Films: Optimizations and Mechanisms. *J. Mater. Chem. C* **2015**, *3*, 5859−5868.

(23) Kim, A.; Won, Y.; Woo, K.; Kim, C.-H.; Moon, J. Highly Transparent Low Resistance ZnO/Ag Nanowire/ZnO Composite Electrode for Thin Film Solar Cells. *ACS Nano* **2013**, *7*, 1081−1091.

(24) Lee, H. J.; Hwang, J. H.; Choi, K. B.; Jung, S.-G.; Kim, K. N.; Shim, Y. S.; Park, C. H.; Park, Y. W.; Ju, B.-K. Effective Indium-Doped Zinc Oxide Buffer Layer on Silver Nanowires for Electrically Highly Stable, Flexible, Transparent, and Conductive Composite Electrodes. *ACS Appl. Mater. Interfaces* **2013**, *5*, 10397−10403.

(25) Choi, K.-H.; Kim, J.; Noh, Y.-J.; Na, S.-I.; Kim, H.-K. Ag Nanowire-Embedded ITO Films as a Near-Infrared Transparent and Flexible Anode for Flexible Organic Solar Cells. *Sol. Energy Mater. Sol. Cells* **2013**, *110*, 147−153.

(26) Lee, M.-S.; Lee, K.; Kim, S.-Y.; Lee, H.; Park, J.; Choi, K.-H.; Kim, H.-K.; Kim, D.-G.; Lee, D.-Y.; Nam, S. W.; Park, J.-U. High-Performance, Transparent, and Stretchable Electrodes Using Graphene−Metal Nanowire Hybrid Structures. *Nano Lett.* **2013**, *13*, 2814−2821.

(27) Moon, I. K.; Kim, J. I.; Lee, H.; Hur, K.; Kim, W. C.; Lee, H. 2D Graphene Oxide Nanosheets as an Adhesive Over-Coating Layer for Flexible Transparent Conductive Electrodes. *Sci. Rep.* **2013**, *3*, 1112.

(28) Yang, S.-B.; Choi, H.; Lee, D. S.; Choi, C.-G.; Choi, S.-Y.; Kim, I.-D. Improved Optical Sintering Efficiency at the Contacts of Silver Nanowires Encapsulated by a Graphene Layer. *Small* **2015**, *11*, 1293−1300.

(29) Preston, C.; Xu, Y.; Han, X.; Munday, J. N.; Hu, L. Optical Haze of Transparent and Conductive Silver Nanowire Films. *Nano Res.* **2013**, *6*, 461−468.

(30) Kim, T.; Canlier, A.; Cho, C.; Rozyyev, V.; Lee, J.-Y.; Han, S. M. Highly Transparent Au-Coated Ag Nanowire Transparent Electrode with Reduction in Haze. *ACS Appl. Mater. Interfaces* **2014**, *6*, 13527−13534.

(31) Rakić, A. D.; Djurišić, A. B.; Elazar, J. M.; Majewski, M. L. Optical Properties of Metallic Films for Vertical-Cavity Optoelectronic Devices. *Appl. Opt.* **1998**, *37*, 5271−5283.

(32) Elman, J. F.; Greener, J.; Herzinger, C. M.; Johs, B. Characterization of Biaxially-Stretched Plastic Films by Generalized Ellipsometry. *Thin Solid Films* **1998**, *313−314*, 814−818.

(33) Lee, K. S.; El-Sayed, M. A. Dependence of the Enhanced Optical Scattering Efficiency Relative to That of Absorption for Gold Metal Nanorods on Aspect Ratio, Size, End-Cap Shape, and Medium Refractive Index. *J. Phys. Chem. B* **2005**, *109*, 20331−20338.